Altered Hepatic and Muscle Substrate Utilization Provoked by GLUT4 Ablation

Mollie Ranalletta,[1] Hua Jiang,[1] Jing Li,[1] T.S. Tsao,[1] Antine E. Stenbit,[1] Masayoshi Yokoyama,[2] Ellen B. Katz,[1] and Maureen J. Charron[1]

Studies were conducted to explore altered substrate utilization and metabolism in GLUT4 null mice. Liver fatty acid synthase mRNA and fatty acid synthesis rates were dramatically increased in GLUT4 null mice compared with control mice and were supported by increased rates of the pentose phosphate pathway oxidative phase and sterol regulatory binding protein mRNA expression. Increased GLUT2 protein content, glucokinase mRNA, and glucose-6-phosphate in GLUT4 null mice may provide substrate for the enhanced fatty acid synthesis. Increased fatty acid synthesis, however, did not lead to hepatic triglyceride accumulation in GLUT4 null mice because of increased hepatic triglyceride secretion rates. GLUT4 null mice rapidly cleared orally administered olive oil, had reduced serum triglyceride concentrations in the fed and the fasted state, and increased skeletal muscle lipoprotein lipase when compared with controls. Oleate oxidation rates were increased in GLUT4 null skeletal muscle in association with mitochondrial hyperplasia/hypertrophy. This study demonstrated that GLUT4 null mice had increased hepatic glucose uptake and conversion into triglyceride for subsequent use by muscle. The ability of GLUT4 null mice to alter hepatic carbohydrate and lipid metabolism to provide proper nutrients for peripheral tissues may explain (in part) their ability to resist diabetes when fed a normal diet. *Diabetes* 54:935–943, 2005

Diabetes is a syndrome of impaired carbohydrate, lipid, and protein metabolism and results in the inability to effectively transport glucose in response to insulin (1–3). The development of diabetes can result from obesity as well as lipodystrophy. The severe loss of adipose tissue is characterized by hypertriglyceridemia, fatty liver, and insulin resistance, which ultimately lead to diabetes. A common factor in the development of diabetes, from both excess and limited adipose tissue, is hypertriglyceridemia (4). Excess triglycerides (TGs) accumulate in inappropriate tissues such as liver, muscle, and pancreas, contributing to insulin resistance and overt diabetes. Use of excess TGs and/or proper storage of TGs may prevent the onset of insulin resistance and/or diabetes.

GLUT4 is the most abundant glucose transporter in insulin-responsive tissues such as skeletal and cardiac muscle and adipose tissue (5). Numerous studies have demonstrated the importance of normal GLUT4 expression and cellular localization in regulating glucose homeostasis (6,7). To better understand mechanisms governing the development of peripheral insulin resistance and hyperglycemia, mice with whole-body knockout of GLUT4 (GLUT4 null) were generated and studied (6,8–13). Notably, these mice are characterized by an 80% reduction in adipose tissue mass and reduced fed serum nonesterified free fatty acids (NEFAs) and fasting ketones (8). Unlike other models of lipodystrophy, GLUT4 null mice do not develop overt diabetes but display severe peripheral insulin resistance, as measured by insulin tolerance tests and glucose uptake into isolated skeletal muscle (8,9). Surprisingly, oral glucose tolerance tests were not different between wild-type and GLUT4 null mice (8). Altered expression and/or targeting of glucose transporters in GLUT4 null muscle did not explain the normal blood glucose levels in GLUT4 null mice (8,10). Combined, data suggested that other compensatory mechanisms were responsible for maintaining glucose homeostasis in GLUT4 null mice.

Liver is responsible for maintaining proper blood glucose levels by sensing hepatoportal glucose, via GLUT2, which is upregulated in GLUT4 null livers (8), and glucokinase (14,15), and regulating gluconeogenesis. We hypothesize that the mechanism(s) for maintaining normal glycemia in GLUT4 null mice may depend on the activity of GLUT2 and subsequent alterations in liver metabolism. Further, we hypothesize that the ability of GLUT4 null mice to resist development of hyperglycemia and dyslipidemia that characterize diabetes may arise from significant alterations in substrate utilization in muscle. The studies reported in the current report were designed to test these hypotheses. Here we demonstrate increased hepatic TG production and secretion and enhanced TG oxidation in skeletal muscle of GLUT4 null mice. These findings suggest that excess fatty acids made by the liver are not used locally but rather are delivered to skeletal muscle as an alternative energy fuel in the absence of

From the [1]Department of Biochemistry, Albert Einstein College of Medicine, Bronx, New York; and the [2]Department of Medicine, Columbia University New York, New York, New York.

Address correspondence and reprint requests to Maureen J. Charron, PhD, Department of Biochemistry, Albert Einstein College of Medicine, 1300 Morris Park Ave., Bronx, NY 10462. E-mail: charron@aecom.yu.edu.

Received for publication 17 September 2004 and accepted in revised form 2 January 2005.

ACC, acetyl-CoA carboxylase; COXIV, cytochrome C oxidase IV; EDL, extensor digitorum longus; G-6-P, glucose-6-phosphate; LPL, lipoprotein lipase; NEFA, nonesterified free fatty acid; PGC-1, PPAR-γ coactivator 1; PiC, inorganic phosphate carrier; PPAR, peroxisome proliferator–activated receptor; TG, triglyceride; UCP, uncoupling protein.

GLUT4. This shift in substrate utilization by both liver and muscle protects GLUT4 null mice from the development of overt hyperglycemia and diabetes.

RESEARCH DESIGN AND METHODS

Female 3- to 4-month-old GLUT4 null mice and sex- and age-matched controls maintained on a C57BL/6J × CBA background were used in this study (8). Animals were fed ad libitum and maintained at a constant temperature (22°C) on a 12-h light and dark cycle. The Animal Care and Use Committee of Albert Einstein College of Medicine in accordance with the Public Health Service Animal Welfare Policy approved all protocols.

Determination of serum glucose, insulin, NEFA, TG, and glycerol levels. Blood from fasted animals was collected after an overnight fast (12 h), and blood from ad libitum–fed mice was collected at ~12:00 A.M. Whole blood was drawn from the orbital sinus and centrifuged. Serum was frozen on dry ice and kept at −70°C until further use. Blood glucose was determined using a glucose meter (Precision Q.I.D., a gift from Abbott Laboratories, Chicago, IL). Serum insulin concentrations were determined using commercially available radioimmunoassays (Linco Research, St. Charles, MO). Serum NEFA levels were measured using a commercial kit from Wako (Wako Chemicals, Neuss, Germany). Serum TG and glycerol concentrations were analyzed using a colorimetric kit (Sigma, St. Louis, MO.).

Hepatic TG production. Mice were fasted for 4 h and then received an intravenous injection of Triton WR1339 (20 mg/200 μl saline). Blood samples were collected before the injections and then every hour for the next 3 h. Serum TG concentration was determined using a colorimetric kit (Sigma). Hepatic TG production was calculated from the 1-h time point and was expressed as micromoles per kilogram per hour.

Oral olive oil loading test. Mice were fasted for 5 h, and then olive oil was delivered by a gavage needle at 16.7 μl/g body wt. Blood samples were obtained immediately before and at 30, 60, 120, 180, and 300 min after oil loading. Serum TG levels were analyzed spectrophotometrically using a kit from Sigma.

Intestinal TG and fatty acid absorption. Absorption studies were performed according to the method reported by Goudriaan et al. (16). The 12- to 14-week-old female control and GLUT4 null mice were fasted overnight for 8–10 h.

Measurement of liver glucose-6-phosphate and glycogen. Animals were sacrificed by cervical dislocation. Livers from GLUT4 null and control mice were freeze-clamped in liquid nitrogen. Small pieces of liver were homogenized in cold 0.3N perchloric acid and centrifuged at 4°C for 10 min at 5,000*g* to remove the fat cake. Cleared homogenate (600 μl) was neutralized by adding 25 μl of 5M K_2CO_3 and centrifuged for 1 min. The supernatant was collected and used for determination of glucose-6-phosphate (G-6-P) and glycogen.

Liver G-6-P content was measured spectrophotometrically as described by Lang and Michal (17). Liver glycogen content was determined using a modified version of the method published by Chan and Exton (18). Briefly, aliquots of supernatant were spotted onto small pieces of Whatman paper. Glycogen was precipitated in 66% ice-cold ethanol. The precipitated glycogen was dissolved in 0.2 mol/l sodium acetate (pH 4.5) and hydrolyzed with amyloglucosidase (Boehringer-Mannheim, Indianapolis, IN). The amount of released glucose was determined using a glucose Trinder kit (Sigma). Glycogen content in liver was expressed as micrograms glucose per milligram wet weight of liver.

Liver TG. Liver TG content was determined using a method previously described (19). Final TG concentration was determined using the TG reagent from Roche (Basel, Switzerland; triglyceride/GB 450032).

Enzyme assays. Acetyl-CoA carboxylase (ACC) activity was assayed in crude liver extracts exactly as previously described (20).

SDS-PAGE and immunoblot analysis. Sample proteins were separated by SDS-PAGE using 5% stacking and 10% resolving gels and then transferred to nitrocellulose filters. Outer mitochondrial membrane proteins were detected using a rabbit polyclonal antibody (1:1,000) (a gift from Dr. P. Scherer, Albert Einstein College of Medicine, Bronx, New York) (21). Relative amounts of serum proteins were quantified using scanning laser densitometry (Molecular Dynamics, Sunnyvale, CA).

Northern blot analysis. Total RNA was isolated using Tri-reagent (Molecular Research Center, Cincinnati, OH) according to the manufacturer's instructions. Approximately 25–50 μg total RNA was loaded onto a 1.2% formaldehyde-agarose gel, transferred to a Hybond–N nylon membrane (Amersham), and hybridized overnight to random primed ^{32}P-labeled cDNA probes under high stringency conditions (50% formamide, 42°C). The filter was washed at 42°C in 2 × sodium chloride and sodium citrate, 1% SDS, and 0.2 × sodium chloride and sodium citrate, 0.1% SDS, solutions and subjected to phosphoimage analysis for visualization and quantification. cDNAs for the following probes were kindly provided by the following: fatty acid synthase, Pascal Ferrè; lipoprotein lipase (LPL), Dr. Ira Goldberg; carnitine palmityl transferase 1, Dr. Daniel P. Kelly; peroxisome proliferator–activated receptor (PPAR)-γ, Dr. Ronald M. Evans; glucokinase, Dr. Mark A. Magnuson; GLUT2, Dr. Bernard Thorens; uncoupling protein (UCP)-2, Dr. Daniel Ricquier; and inorganic phosphate carrier (PiC), Dr. Philipp E. Scherer. Fragments for the murine sterol regulatory binding protein were generated using the following primers: 5′-GCCAACTCTCCTGAGAGCTT-3′ and 5′-CTCCTGCTTGAGCTTCTGGTT-3′. UCP-3 and cytochrome C oxidase IV (COX IV) cDNAs were subcloned by RT-PCR using the primer sequences reported by Combatsiaris and Charron (22). Normalization of gel loading was performed by re-probing filters with an oligonucleotide specific for 18S rRNA and end labeled by T4 polynucleotide kinase.

Pentose phosphate pathway. Activity of the pentose phosphate pathway was determined spectrophotometrically by measuring the release of NADPH according to the method described by Cabezas et al. (23). Data are reported as micromoles of NADPH produced per minute per milligram protein.

Fatty acid synthesis rates. Fatty acid synthesis rates were determined according to the method described by Lin et al. (24). Mice were tail vein injected with 30 μCi ^{14}C-acetate (Amersham catalog number CFA13) in the fed state. After 1 h, mice were killed, and liver tissue was harvested. Data are presented as disintegrations per minute per hour per milligram tissue.

Serum LPL activity. Hepatic and peripheral (white adipose and muscle) LPL activity was determined according to the method of Iverius and Ostlund-Lindqvist (25). Mice were tail vein injected with either saline or heparin (200 units/mouse; Sigma), and blood was collected 30 min later from the orbital sinus. Then, 10 μl serum was used with high (1 mol/l) or low (150 mmol/l) NaCl present in the buffer to determine hepatic and total lipase activity, respectively. Data are reported as nanomoles free fatty acid per milligram protein per minute.

Muscle LPL activity. LPL activity in quadriceps from control and GLUT4 null mice was determined according to the method of Hocquette et al. (26). Data are reported as counts per minute per milligram tissue.

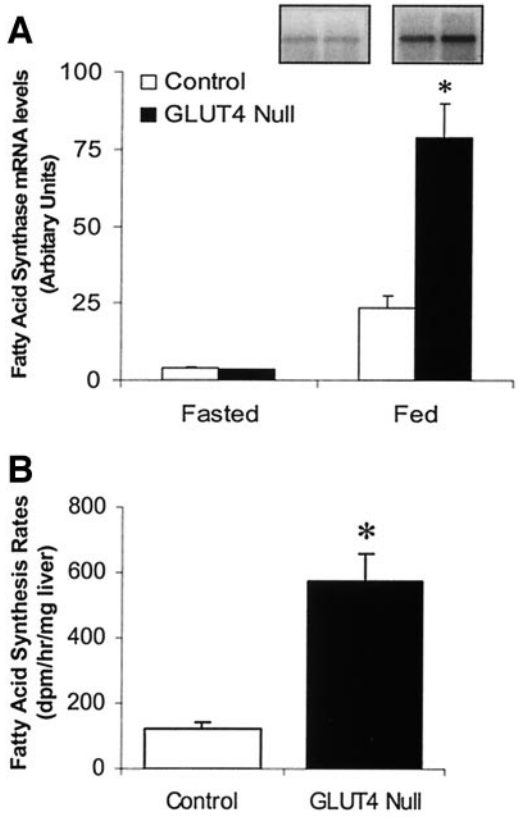

FIG. 1. *A*: Liver fatty acid synthase mRNA expression. Blots were normalized by hybridization with 18S ribosomal RNA (rRNA) (data not shown). Results of n = 5–11 under fed conditions for both genotypes were quantified by phosophorimage analysis. *B*: Liver fatty acid synthesis rates. Data are means ± SE for n = 6–7 per group. Data are reported as the incorporation rate of ^{14}C-acetate into fatty acids per hour per milligram liver. *P < 0.001 when comparing control and GLUT4 null mice.

TABLE 1
Serum metabolites and liver composition

	Fed		Fasted	
	Control	GLUT4 null	Control	GLUT4 null
Serum				
n	18–20	22	9	10
Glucose (mg/dl)	125.5 ± 5.43	150.7 ± 4.64*	84.22 ± 7.08	127.1 ± 7.88*
Insulin (ng/ml)	1.67 ± 0.02	3.99 ± 0.60*	Not measured	Not measured
TGs (mg/dl)	135.63 ± 11.33	62.86 ± 3.93*	69.77 ± 4.73	37.62 ± 5.86†
Glycerol (mg/dl)	6.30 ± 0.77	13.67 ± 2.02†	19.63 ± 3.40	16.61 ± 1.89
NEFAs (mEq/l)	1.21 ± 0.05	0.94 ± 0.03*	1.71 ± 0.08	1.26 ± 0.07*
Liver metabolites				
n	5–8	5–8	4–6	5–6
Glycogen (μg/mg tissue)	28.69 ± 3.72	20.49 ± 4.03	0.845 ± 0.51	0.380 ± 0.38
TGs (μg/mg tissue)	3.66 ± 0.95	4.15 ± 1.57	28.41 ± 2.82	29.24 ± 2.50
G-6-P (μmol/g wet wt)	1.51 ± 0.09	1.90 ± 0.12†	0.72 ± 0.06	0.18 ± 0.02*
Liver mRNA				
n	5–11	5–11		
PPAR-γ mRNA (arbitrary units)	1.55 ± 0.16	2.76 ± 0.37†		
GLUT2 mRNA (arbitrary units)	0.028 ± 0.001	0.059 ± 0.003*		
Glucokinase mRNA (arbitrary units)	9.00 ± 1.14	18.16 ± 0.69		
SREBP mRNA (arbitrary units)	0.205 ± 0.012	0.309 ± 0.024*		

Data are means ± SE. Total RNA (25 μg) extracted from liver was loaded into each lane and normalized by hybridization with 18S ribosomal RNA (rRNA). Results were quantified by phosophorimage analysis. SREBP, sterol regulatory binding protein. *$P < 0.001$, GLUT4 null vs. control; †$P < 0.05$, GLUT4 null vs. control.

Oleate oxidation in soleus and extensor digitorum longus. Individual soleus and extensor digitorum longus (EDL) muscles from 10- to 14-week-old mice were isolated and preincubated for 15 min in Krebs-Ringer buffer supplemented with 4% BSA (fraction V, RIA grade from Sigma), 0.5 mmol/l oleate, and 5 mmol/l glucose. Muscle was then transferred to new vials containing the same buffer plus 0.8 μCi/ml [1-^{14}C]oleic acid (60 mCi/mmol, Amersham) and incubated for 45 min. Samples were acidified with 15% perchloric acid, and the CO_2 was captured on Whatman paper suspended within the vials. ^{14}C radioactivity was quantitated after overnight quenching at 4°C by liquid scintillation counting. Data are reported as nanomoles oleate per gram wet muscle weight per 45 min.

Transmission electron microscopy. Soleus and EDL muscles were isolated and fixed in 2.5% gluteraldehyde in 0.1 mol/l cacodylate buffer, postfixed with 1% osmium tetroxide followed by 1% uranyl acetate, dehydrated through a graded series of ethanol and embedded in LX112 resin (LADD Research Industries, Burlington, VT). Ultrathin sections were cut on a Reichaert Ultracut E microtome, stained with uranyl acetate followed by lead citrate, and viewed on a JEOL 1200EX transmission electron microscope at 80 kV. Representative micrographs were taken at 10,000× magnification.

Statistical analysis. Statistical comparison of control versus GLUT4 null mice was done using the unpaired two-tailed Student's *t* test. Data are means ± SE for each group. Significance was accepted at $P < 0.05$.

RESULTS

Increased fatty acid synthesis in GLUT4 null liver. Northern blot analysis of liver revealed a 3.3-fold ($P < 0.002$) increase in fatty acid synthase mRNA in fed but not fasted GLUT4 null mice compared with control mice (Fig. 1*A*). The overall rates of fatty acid synthesis, as measured by incorporation of ^{14}C-acetate into liver fatty acids, revealed a sixfold increase in fatty acid synthesis in GLUT4 null compared with control mice (Fig. 1*B*). Regulators of lipid metabolism were also measured. An elevated level of PPAR-γ is associated with upregulation of ACC and fatty acid synthase leading to TG accumulation. GLUT4 null mice have significantly higher (1.8-fold, $P < 0.02$) expression levels of PPAR-γ mRNA compared with control mice in the fed state (Table 1). As expected, ACC activity is also increased 1.8- and 1.2-fold in GLUT4 null mice compared with control mice in the fed and fasted

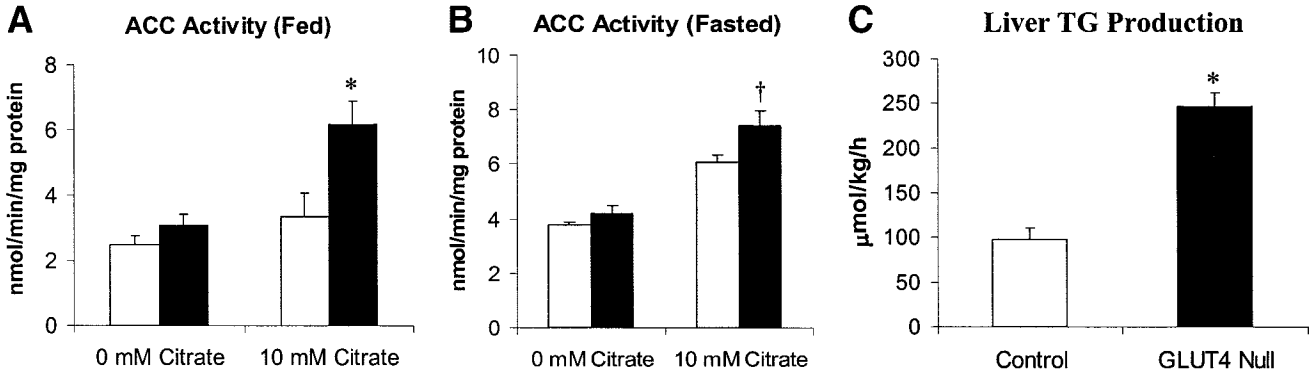

FIG. 2. Basal (0 mmol/l citrate) and citrate-dependent (10 mmol/l citrate) ACC activity in GLUT4 null and control liver under fed (*A*) and fasted (*B*) conditions. Data are means ± SE for $n = 5$ mice per group. ACC activity is expressed as nanomoles of ^{14}C transferred to acetyl-CoA per minute per milligram protein. *$P < 0.01$ and †$P < 0.05$ when comparing control (□) and GLUT4 null (■) mice. *C*: Liver TG production. Fasted mice received an intravenous injection containing 20 mg Triton WR 1339 to inhibit TG clearance. Serum TGs were measured as described in RESEARCH DESIGN AND METHODS. Data are means ± SE for $n = 4$–5 per group. *$P < 0.001$ when comparing control and GLUT4 null mice.

states under stimulated conditions (10 mmol/l citrate), respectively (Fig. 2*A* and *B*). The overall TG content in liver was not different in GLUT4 null mice compared with control mice in the fed and fasted states (Table 1). Genes involved in hepatic fatty acid utilization were examined. There were no differences in expression of LPL (8.20 ± 0.62 vs. 8.25 ± 1.31 arbitrary units, $n = 5$ mice per group) in liver from fed GLUT4 null and control mice, respectively. The transport of long-chain fatty acyl-CoA into the mitochondria for oxidation is regulated by carnitine palmityl transferase 1. There was no difference in expression levels of carnitine palmityl transferase 1 (5.14 ± 0.59 vs. 4.47 ± 0.47 arbitrary units, $n = 5$ mice per group) in liver of fed GLUT4 null or control mice, respectively. These data suggest that fatty acid oxidation is not altered in GLUT4 null liver because of normal levels of fatty acid transport into liver and mitochondria in the fed state. Hepatic TG secretion rates, on the other hand, were increased 2.5-fold ($P < 0.001$) in GLUT4 null mice compared with control mice (Fig. 2*C*). Collectively these data demonstrate increased hepatic fatty acid synthesis and secretion in GLUT4 null mice.

Increased activation of the pentose phosphate pathway in GLUT4 null liver. Fatty acid synthesis requires the generation of NADPH by the pentose phosphate pathway. Levels of the oxidative and nonoxidative branches were measured by analyzing NADPH release from liver homogenates. The oxidative and nonoxidative branches were significantly increased in GLUT4 nulls, 1.6-fold ($P < 0.001$) and 1.4-fold ($P < 0.05$), respectively (Fig. 3*A*). The ratio of oxidative to nonoxidative activity was not significantly different between GLUT4 null and control mice, indicating that they equally recycle ribose for NADPH production (Fig. 3*B*). However, the difference between the oxidative and nonoxidative branches was significantly increased—1.8-fold ($P < 0.001$) in GLUT4 nulls, indicating a high rate of ribose production that is consistent with tissues undergoing increased fatty acid synthesis (Fig. 3*B*). These data support the observed increase in fatty acid synthesis rates observed in GLUT4 null liver.

Increased glucose phosphorylation in GLUT4 null livers. While GLUT4 null mice have small elevations in circulating glucose and insulin, they do not develop diabetes on normal pellet diet (Table 1). As previously reported (8), GLUT4 null mice have a 1.7-fold increase in the mRNA expression of GLUT2 in liver when compared with age- and sexed-matched control mice. Hepatic GLUT2 mRNA expression was increased 2.1-fold ($P < 0.001$) in fed GLUT4 null mice (Table 1). The initial step of glycolysis, glucose phosphorylation, is regulated by glucokinase in liver. During the fed state, glucokinase expression was increased twofold ($P < 0.001$) in GLUT4 null mice compared with control mice, but showed no difference in the fasted state (data not shown; Table 1). The product of glucokinase, G-6-P, was also elevated 1.3-fold ($P < 0.05$) in fed GLUT4 null mice, but decreased fourfold ($P < 0.001$) with fasting (Table 1). The transcription factor sterol regulatory binding protein, which has been shown to activate glucokinase transcription and inhibit PEPCK transcription (27), was significantly upregulated 1.5-fold ($P < 0.01$) in fed GLUT4 null liver (Table 1). Overall glycogen content was not significantly different in GLUT4 null liver compared with control mice in the fed state (Table 1). GLUT4 null liver also showed normal mRNA expression of PEPCK (7.17 ± 0.34 vs. 6.34 ± 0.23 arbitrary units, $n = 5$ per group) and glucose-6-phosphatase (9.46 ± 1.65 vs. 7.43 ± 1.20 arbitrary units, $n = 5$ per group) in the fed state when compared with control mice. Together these data suggest that during feeding, when circulating glucose and insulin become elevated, the GLUT4 null liver significantly increases glucose uptake and glycolysis compared with control liver, but maintain normal hepatic glycogen content.

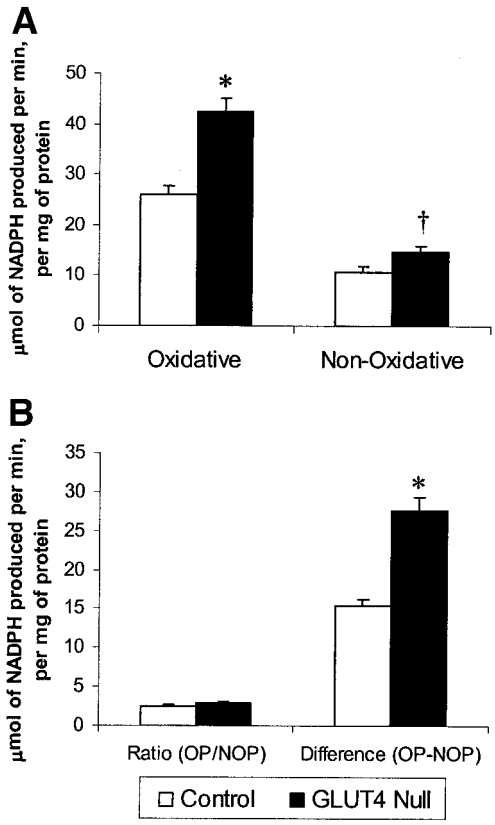

FIG. 3. Liver pentose phosphate pathway activity. Liver homogenates from fed control ($n = 5$) and GLUT4 null ($n = 5$) female mice were analyzed for oxidative and nonoxidative pentose phosphate pathway activity (*A*). The ratio and differences in the oxidative (OP) and nonoxidative (NOP) branch are represented in *B*. *$P < 0.001$ and †$P < 0.05$ when comparing control and GLUT4 null mice.

Increased fatty acid oxidation in GLUT4 null muscle. The ability of GLUT4 null mice to use lipids was assessed by oral administration of olive oil. GLUT4 null mice showed an enhanced ability to clear orally administered lipids (Fig. 4*A*). However, GLUT4 null mice show no difference compared with control mice in their ability to absorb TGs or fatty acids (Fig. 4*B* and *C*). Serum levels of NEFAs were reduced 1.3-fold ($P < 0.001$) and 1.4-fold ($P < 0.001$) in the fed and fasted states, respectively, in the GLUT4 null mice compared with control mice (Table 1). Fed and fasted serum TGs were reduced 2.2-fold ($P < 0.001$) and 1.9-fold ($P < 0.05$), respectively, in GLUT4 null mice compared with control mice (Table 1). Fatty acid oxidation by muscle and adipose tissue requires the breakdown of serum TGs into NEFAs through the action of LPL. Serum levels of total LPL (63.0 ± 2.4 and 66.8 ± 2.8 nmol free fatty acid · mg^{-1} protein · min^{-1}, $n = 5$ per group) and

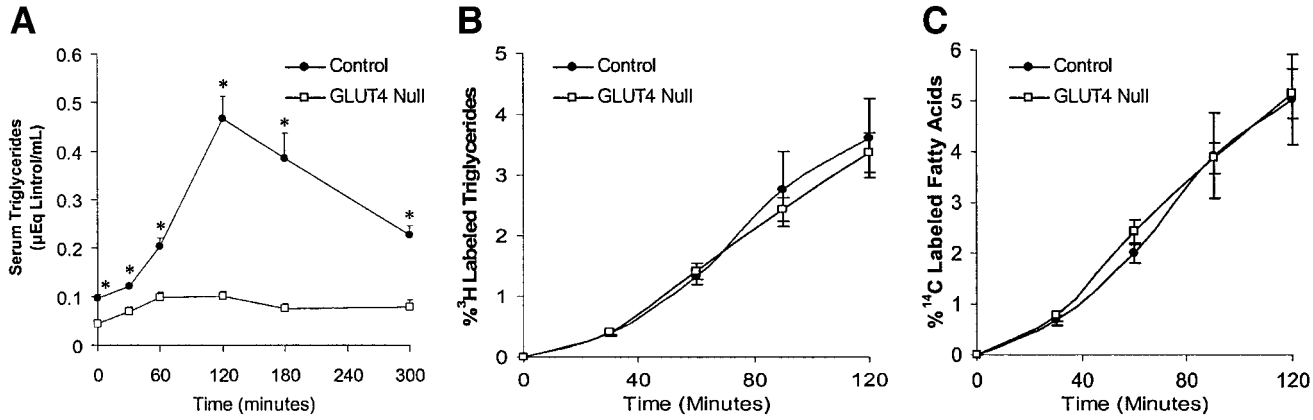

FIG. 4. *A*: **Oral olive oil challenge. Each mouse received 16.7 μl olive oil/g body wt. Results are an average of five mice per group. Serum TGs were measured as described in RESEARCH DESIGN AND METHODS. TG (*B*) and fatty acid (*C*) intestinal absorption is shown. After an overnight fast, mice were tail vein injected with Triton WR 1339 to inhibit LPL activity, followed by an oral bolus of olive oil containing 7 μCi glycerol-[^{3}H]-oleate and 2 μCi[9,10(n)-^{14}C] palmitic acid. n = 7 mice per genotype.**

hepatic LPL (11.3 ± 0.39 and 11.0 ± 0.82 nmol free fatty acid · mg^{-1} protein · min^{-1}, n = 5 per group) were not significantly different (P = 0.2 and P = 0.7) between control and GLUT4 null mice, respectively, in the fed state. Northern blot analysis from gastrocnemius muscle revealed a 1.6-fold ($P < 0.01$) increase in LPL mRNA in fed GLUT4 null mice compared with controls (Fig. 5*A*). Muscle LPL activity was increased 2.1-fold ($P < 0.001$) in GLUT4 null mice compared with control mice (Fig. 5*B*).

Based on the findings of increased hepatic TG production and increased muscle LPL activity, we next examined the ability of GLUT4 null muscle to oxidize TGs. Oleate oxidation rates in the GLUT4 null soleus and EDL muscles were increased 1.5-fold ($P < 0.05$) and 1.3-fold ($P < 0.05$), respectively (Fig. 5*C* and *D*). This coincides with mitochondrial hypertrophy/hyperplasia noted in transmission electron micrographs of GLUT4 null soleus and EDL muscle (Fig. 6*A*). Mitochondrial hypertrophy was accompanied by increased expression of mitochondrial outer membrane proteins (Fig. 6*B*). The average increase was ~1.8-fold in soleus and 1.4-fold in EDL of GLUT4 null mice relative to control mice ($P < 0.01$). Expression of genes encoding the inner mitochondrial membrane proteins COX IV and PiC were increased 30 and 50%, respectively, in GLUT4 null skeletal muscle compared with control mice ($P < 0.01$) (Fig. 6*C*). UCP-2 mRNA levels were not altered in GLUT4 null skeletal muscle relative to controls, but UCP-3 mRNA levels were reduced 50% in GLUT4 null muscle compared with control ($P < 0.01$) (Fig. 6*C*).

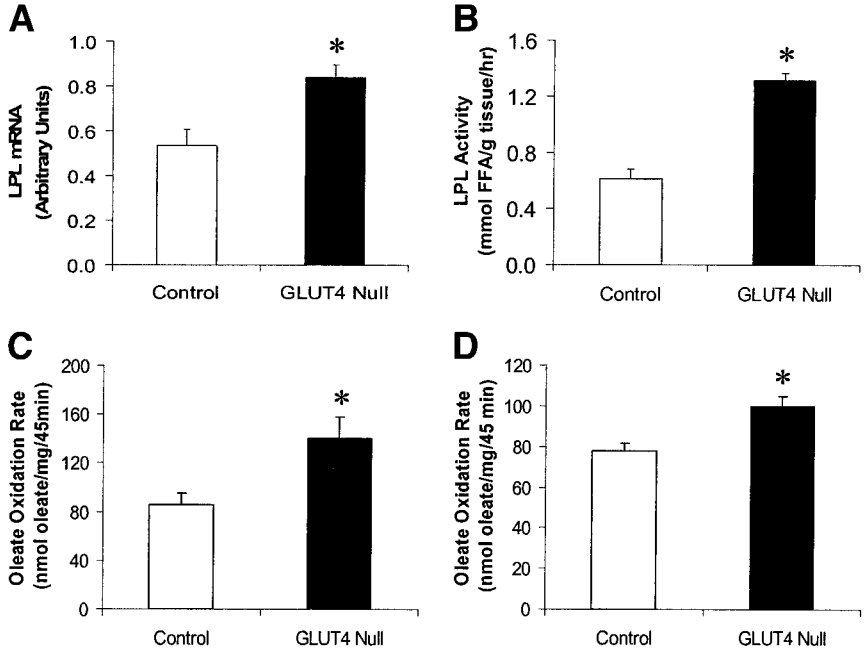

FIG. 5. Skeletal muscle LPL mRNA expression and activity. Total RNA (25 μg) extracted from gastrocnemius muscle was loaded into each lane and normalized by hybridization with 18S ribosomal RNA (rRNA). Results (means ± SE arbitrary units) under fed conditions were quantified by phosophorimage analysis of n = 10 mice per genotype (*A*). LPL activity was measured in quadriceps muscles (values are means ± SE for n = 5 mice per genotype) after an overnight fast (*B*). *$P < 0.01$ when comparing control and GLUT4 null. Oleate oxidation rates in isolated soleus (*C*) and EDL (*D*) muscle are shown. Muscles were isolated from control and GLUT4 null mice, and oxidation was measured as described in RESEARCH DESIGN AND METHODS. Data are means ± SE for n = 9 per group. *$P < 0.05$ when comparing control and GLUT4 null mice. FFA, free fatty acid.

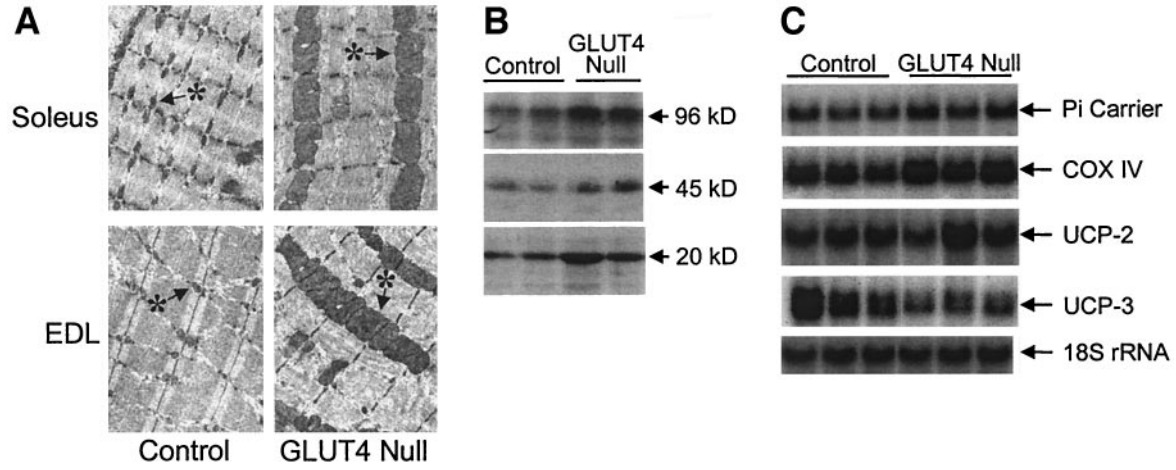

FIG. 6. ***A*****: Transmission electron micrographs of mitochondria from soleus and EDL muscle from GLUT4 null and control mice. Representative micrographs are shown at 10,000× magnification. *Mitochondria.** ***B*****: Representative immunoblot analysis of mitochondrial outer membrane proteins in soleus muscle. A total of 100 μg total muscle was separated by 10% SDS-PAGE and transferred to nitrocellulose for immunoblot analysis. Three predominant bands migrated at the molecular weights indicated were quantified from control and GLUT4 null mice (six muscles per group).** ***C*****: Northern blot analysis of mitochondrial inorganic phosphate (Pi) carrier and COXIV, UCP-2, and UCP-3 gene expression. Total RNA (40 μg) was extracted from hindlimb muscles of control and GLUT4 null mice and loaded into each lane. Blots were normalized to 18S rRNA. Results of $n = 6$ for each group were quantified by phosphoimage analysis.**

DISCUSSION

GLUT4 null mice have invoked compensatory mechanisms in the absence of GLUT4 that allow them to resist diabetic hyperglycemia in the absence of GLUT4. The liver senses hepatoportal glucose concentrations in a GLUT2-dependent manner and adjusts glucose influx and efflux accordingly to maintain euglycemia (14). In GLUT4 null mice, GLUT2 is increased to promote increased influx and thus clearance of glucose from serum. Glucose influx correlates with increased levels of glucokinase mRNA, the first step in glycolysis, and increased generation of G-6-P. Transgenic mice overexpressing glucokinase have reduced fasting glucose levels, improved glucose tolerance, and increased hepatic glycogen (28). Chronic glucokinase overexpression (>6 months) results in glucose intolerance, hyperglycemia, hyperinsulinemia, and hypertriglyceridemia (29). Therefore, although glucokinase appears to be beneficial in lowering blood glucose concentrations, prolonged overexpression leads to lipid storage problems due to continual hepatic lipogenesis. Enhanced TG utilization by muscle protects GLUT4 null mice from the detrimental effects of chronic hepatic lipogenesis seen in older glucokinase transgenic mice.

Increased glucose flux into GLUT4 null liver leads to increased G-6-P concentrations. G-6-P is a potent stimulator of fatty acid synthesis, as demonstrated by in vitro experiments with cultured rat hepatocytes (30). Both the oxidative branch of the pentose phosphate pathway and fatty acid synthesis are increased in GLUT4 null mice in the fed state. PPAR-γ promotes transcription of genes associated with lipid storage and is upregulated in GLUT4 null liver. Increased fatty acid synthesis is often associated with activation of the transcription factor PPAR-γ in response to thiazolidinediones treatment. In general, levels of PPAR-γ are low in liver (10–30% of what is seen in adipose tissue) (31) but are increased in several mouse models of hepatic steatosis (32). Liver-specific inactivation of PPAR-γ reduced hepatic steatosis by 30% in lipoatrophic A-ZIP/FI (AZIP) fatless mice but impaired TG clearance and increased muscle TG storage (33). AZIP mice without PPAR-γ were more diabetic, presumably because of increased peripheral insulin resistance. Similarly, disruption of PPAR-γ in liver of leptin-deficient mice results in reduced hepatic steatosis but increased serum TGs and free fatty acids and the severity of diabetes (34). In models of reduced PPAR-γ, liver steatosis was improved, but peripheral insulin sensitivity was worsened because of increased storage of TGs in muscle and adipose tissue. GLUT4 null mice resist the deleterious effects of increased hepatic fatty acid synthesis through enhanced TG clearance and oxidation in skeletal muscle. Muscle-specific inactivation of PPAR-γ results in increased adiposity with normal insulin sensitivity in muscle but whole-body insulin resistance due to hepatic insulin resistance (35). Collectively, these mouse models demonstrate that alteration of PPAR-γ in liver or muscle has systemic effects on both glucose and lipid metabolism. GLUT4 null mice overcome severe peripheral insulin resistance by altering liver metabolism in a way that complements alterations in skeletal muscle substrate utilization.

Despite increased hepatic fatty acid synthesis and low adipose tissue mass, GLUT4 null mice have reduced serum TG levels. The clearance of serum TGs is greatly accelerated in GLUT4 null mice and is suggestive of enhanced fatty acid clearance and oxidation. Based on the phenotype of GLUT4 null mice, excess hepatic-derived TGs are not stored in adipose tissue (GLUT4 null mice have an 80% reduction in adipose tissue mass). Proper storage of TGs is essential for the maintenance of insulin sensitivity. Accumulation of TGs in nonadipose tissues such as skeletal muscle, liver, and/or pancreas can result in the development of insulin resistance and diabetes (36). Serum TGs are cleared through the activation of LPL. Serum LPL and hepatic lipase activity were not altered in GLUT4 null mice, but skeletal muscle LPL mRNA levels and activity were significantly increased. Transgenic mice overexpressing human LPL have reduced serum TGs and are protected from diet-induced hypertriglyceridemia (37).

Overexpression of LPL specifically in skeletal muscle increased muscle TG content, decreased insulin-stimulated glucose uptake into muscle, and caused skeletal muscle mitochondrial hyperplasia/hypertrophy (38,39). In combination with increased LPL activity, GLUT4 null skeletal muscles also exhibit enhanced rates of oleate oxidation, which may protect them from the adverse effects of intramyocellular TGs. Future studies will be conducted to determine the direct contribution of hepatic-derived fatty acid particles to the increased β-oxidation observed in GLUT4 null mice during the fed state.

GLUT4 null mice display skeletal muscle mitochondrial hyperplasia/hypertrophy associated with increased oleate oxidation, although the direct contribution of lipid uptake was not measured. The observed mitochondrial hypertrophy is confirmed by increased expression of outer mitochondrial membrane proteins. The hypertrophied mitochondria most likely embody an increased capability to undergo oxidative phosphorylation. This is strongly supported by increased expression of inorganic phosphate carrier and COX IV mRNA in muscle (40). COX IV is one of the major rate-limiting factors in the mitochondrial respiratory chain, and its activity has been positively correlated with pyruvate and palmitate oxidation rates (41,42). PiC is an inner mitochondrial membrane protein that transports inorganic phosphate into the mitochondrial matrix, where it serves as substrate for ATP synthesis (43). Decreased expression of UCP-3 should complement the increased capacity for substrate oxidation to preserve a normal energetic state in GLUT4 null skeletal muscle. This is supported by results from Tsuboyama-Kasaoka et al. (44) demonstrating that increased glucose flux in skeletal muscle after GLUT4 overexpression led to increased UCP-3 expression and oxygen consumption. UCP-3 knockout mice have a fourfold increase in skeletal muscle ATP synthesis with no change in the tricarboxylic acid cycle, demonstrating increased mitochondrial energy coupling (45).

The molecular mechanism(s) responsible for mitochondrial alterations seen in the absence of insulin-stimulated flux of glucose through GLUT4 are not fully understood. Mitochondrial proliferation and increased fatty acid oxidation are also characteristics of endurance-trained athletes (46). PPAR-γ coactivator 1 (PGC-1) regulates transcription factors involved in mitochondrial biogenesis (47). Skeletal muscle transgenic overexpression of PGC-1 caused conversion of fast-twitch glycolytic fibers to slow-twitch oxidative fibers and, in the highest transgenic expressing line, had decreased body weight (48). Consistent with increased oleate oxidation, GLUT4 null tibialis anterior and EDL muscles have increased fast-twitch oxidative type IIA fibers and reduced fast-twitch glycolytic type IIB fibers (12). Mice with transgenic overexpression of a related protein, PGC-1b, were lean, hyperphagic, and resistant to diet-induced obesity because of increased energy expenditure (49). A key regulator of fatty acid synthesis and oxidation is ACC. ACC2-deficient mice have increased fatty acid oxidation rates and accumulate less fat than control mice (50). Interestingly, these mice, like GLUT4 nulls, have increased fatty acid oxidation in soleus muscle. However, unlike GLUT4 nulls, the liver of ACC2-deficient mice exhibits increased fatty acid oxidation.

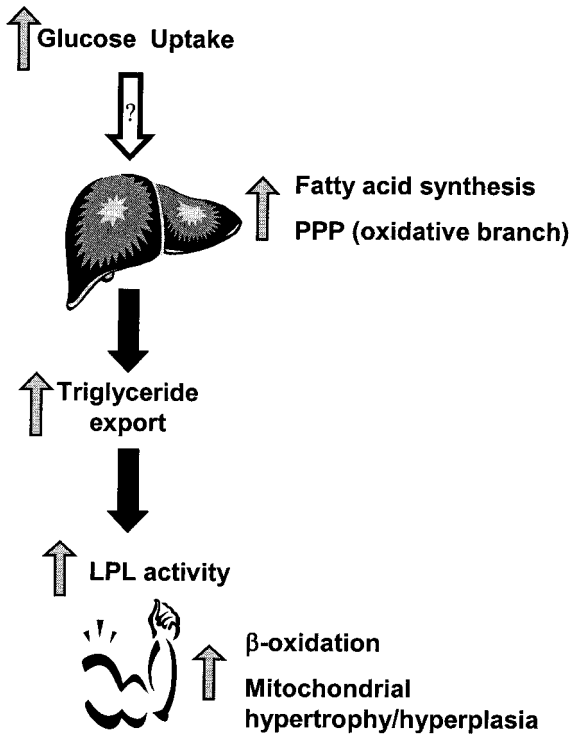

FIG. 7. Schematic overview of altered hepatic and muscle metabolism in GLUT4 null mice. Liver glucose uptake is enhanced because of an upregulation in GLUT2 and glucokinase. This leads to increases in liver glycolysis, fatty acid synthesis, and the oxidative branch of the pentose phosphate pathway (PPP). GLUT4 null mice have an enhanced ability to clear serum TGs, suggesting increased peripheral TG utilization in the absence of GLUT4. Collectively these alterations provide an alternative use for excess circulating glucose that would normally be cleared by GLUT4 and thereby protect the animal from hyperglycemia.

When challenged with a high-fat diet, ACC2-deficient mice gained less weight than controls and were protected from development of diabetes (50). Malonyl-CoA at high concentrations promotes fatty acid synthesis and inhibits β-oxidation. Malonyl-CoA concentrations in GLUT4 null gastrocnemius muscle were not different from control mice (data not shown). In GLUT4 null mice, increased skeletal muscle fatty acid oxidation complements increased liver fatty acid synthesis and prevents the accumulation of intramyocellular TGs. This alteration in substrate utilization also provides fuel for high-energy phosphate formation in the absence of significant insulin-stimulated glucose utilization. Whether the alterations in substrate utilization noted in GLUT4 null mice modulate overall energy expenditure require additional studies.

Data presented here clearly demonstrate the significance of coordinated alterations in substrate utilization as a major compensatory mechanism invoked by GLUT4 null mice for maintenance of euglycemia. The liver plays a critical role in glucose clearance and in providing alternative energy substrates (TGs) for use by peripheral tissues such as skeletal muscle. Skeletal muscle, through increased mitochondrial hypertrophy/hyperplasia and oxidative capacity, is able to rapidly clear and use serum TGs and prevent their accumulation in nonadipose depots. A schematic representation of the adaptations in GLUT4 null liver and skeletal muscle substrate utilization as a means to manage the potential diabetic effects of global GLUT4 ablation are presented in Fig. 7. New therapeutic ap-

proaches for the treatment of diabetes should consider the interactions of lipid and glucose metabolism and cross-talk that occurs among tissues.

ACKNOWLEDGMENTS

This work was supported by grants from the National Institutes of Health (NIH) (DK47425 and HL58119), American Diabetes Association, Comprehensive Cancer Center of the Albert Einstein College of Medicine, and the Diabetes Research and Training Center. M.R., T.S.T., and A.E.S. were supported by NIH (5T32DK07513, 5T32HL07675, and 5T32GM07491, respectively).

We wish to acknowledge the following individuals: Dr. Juleen Zierath for helpful advice with the oleate oxidation studies; Dr. Clay Semenkovich, Trey Coleman, and Dr. Ira Goldberg for providing technical guidance for LPL measurements; Dr. Peter Voshol for advice on intestinal lipid absorption measurements and manuscript preparation; Leslie Gunter for transmission electron microscopy; Drs. Sally Du and Lingguang Cui for mouse assistance; and Drs. Ann Louise Olson, Luciano Rossetti, and Philipp Scherer for valuable discussions and critical reading of the manuscript.

This work was submitted in partial fulfillment of the requirements for the PhD degree for the Albert Einstein College of Medicine (M.R.).

REFERENCES

1. Bonadonna RC, Saccomani MP, Seely L, Zych KS, Ferrannini E, Cobelli C, DeFronzo RA: Glucose transport in human skeletal muscle: the in vivo response to insulin. *Diabetes* 42:191–198, 1993
2. Rothman DL, Shulman RG, Shulman GI: 31P nuclear magnetic resonance measurements of muscle glucose-6-phosphate: evidence for reduced insulin-dependent muscle glucose transport or phosphorylation activity in non-insulin-dependent diabetes mellitus. *J Clin Invest* 89:1069–1075, 1992
3. Rothman DL, Magnusson I, Cline G, Gerard D, Kahn CR, Shulman RG, Shulman GI: Decreased muscle glucose transport/phosphorylation is an early defect in the pathogenesis of non-insulin-dependent diabetes mellitus. *Proc Natl Acad Sci U S A* 92:983–987, 1995
4. Julius U: Influence of plasma free fatty acids on lipoprotein synthesis and diabetic dyslipidemia. *Exp Clin Endocrinol Diabetes* 111:246–250, 2003
5. Charron MJ, Brosius FC 3rd, Alper SL, Lodish HF: A glucose transport protein expressed predominately in insulin-responsive tissues. *Proc Natl Acad Sci U S A* 86:2535–2539, 1989
6. Charron MJ, Katz EB, Olson AL: GLUT4 gene regulation and manipulation. *J Biol Chem* 274:3253–3256, 1999
7. Wallberg-Henriksson H, Zierath JR: GLUT4: a key player regulating glucose homeostasis? Insights from transgenic and knockout mice (Review). *Mol Membr Biol* 18:205–211, 2001
8. Katz EB, Stenbit AE, Hatton K, DePinho R, Charron MJ: Cardiac and adipose tissue abnormalities but not diabetes in mice deficient in GLUT4. *Nature* 377:151–155, 1995
9. Stenbit AE, Burcelin R, Katz EB, Tsao TS, Gautier N, Charron MJ, Le Marchand-Brustel Y: Diverse effects of Glut 4 ablation on glucose uptake and glycogen synthesis in red and white skeletal muscle. *J Clin Invest* 98:629–634, 1996
10. Ryder JW, Kawano Y, Chibalin AV, Rincon J, Tsao TS, Stenbit AE, Combatsiaris T, Yang J, Holman GD, Charron MJ, Zierath JR: In vitro analysis of the glucose-transport system in GLUT4-null skeletal muscle. *Biochem J* 342:321–328, 1999
11. Ryder JW, Kawano Y, Galuska D, Fahlman R, Wallberg-Henriksson H, Charron MJ, Zierath JR: Postexercise glucose uptake and glycogen synthesis in skeletal muscle from GLUT4-deficient mice. *FASEB J* 13:2246–2256, 1999
12. Gorselink M, Drost MR, de Brouwer KF, Schaart G, van Kranenburg GP, Roemen TH, van Bilsen M, Charron MJ, van der Vusse GJ: Increased muscle fatigability in GLUT-4-deficient mice. *Am J Physiol Endocrinol Metab* 282:E348–E354, 2002
13. Jiang H, Li J, Katz EB, Charron MJ: GLUT4 ablation in mice results in redistribution of IRAP to the plasma membrane. *Biochem Biophys Res Commun* 284:519–525, 2001
14. Burcelin R, Dolci W, Thorens B: Glucose sensing by the hepatoportal sensor is GLUT2-dependent: in vivo analysis in GLUT2-null mice. *Diabetes* 49:1643–1648, 2000
15. Postic C, Shiota M, Magnuson MA: Cell-specific roles of glucokinase in glucose homeostasis. *Recent Prog Horm Res* 56:195–217, 2001
16. Goudriaan JR, Dahlmans VE, Febbraio M, Teusink B, Romijn JA, Havekes LM, Voshol PJ: Intestinal lipid absorption is not affected in CD36 deficient mice. *Mol Cell Biochem* 239:199–202, 2002
17. Lang G, Michal G: *Methods of Enzymatic Analysis.* Vol. 3. New York, Academic, 1974
18. Chan TM, Exton JH: A rapid method for the determination of glycogen content and radioactivity in small quantities of tissue or isolated hepatocytes. *Anal Biochem* 71:96–105, 1976
19. Carr TP, Andresen CJ, Rudel LL: Enzymatic determination of triglyceride, free cholesterol, and total cholesterol in tissue lipid extracts. *Clin Biochem* 26:39–42, 1993
20. Kudo N, Barr AJ, Barr RL, Desai S, Lopaschuk GD: High rates of fatty acid oxidation during reperfusion of ischemic hearts are associated with a decrease in malonyl-CoA levels due to an increase in 5′-AMP-activated protein kinase inhibition of acetyl-CoA carboxylase. *J Biol Chem* 270:17513–17520, 1995
21. Scherer PE, Lisanti MP, Baldini G, Sargiacomo M, Mastick CC, Lodish HF: Induction of caveolin during adipogenesis and association of GLUT4 with caveolin-rich vesicles. *J Cell Biol* 127:1233–1243, 1994
22. Combatsiaris TP, Charron MJ: Downregulation of uncoupling protein 2 mRNA in white adipose tissue and uncoupling protein 3 mRNA in skeletal muscle during the early stages of leptin treatment. *Diabetes* 48:128–133, 1999
23. Cabezas H, Raposo RR, Melendez-Hevia E: Activity and metabolic roles of the pentose phosphate cycle in several rat tissues. *Mol Cell Biochem* 201:57–63, 1999
24. Lin X, Schonfeld G, Yue P, Chen Z: Hepatic fatty acid synthesis is suppressed in mice with fatty livers due to targeted apolipoprotein B38.9 mutation. *Arterioscler Thromb Vasc Biol* 22:476–482, 2002
25. Iverius PH, Ostlund-Lindqvist AM: Preparation, characterization, and measurement of lipoprotein lipase. *Methods Enzymol* 129:691–704, 1986
26. Hocquette JF, Graulet B, Olivecrona T: Lipoprotein lipase activity and mRNA levels in bovine tissues. *Comp Biochem Physiol B Biochem Mol Biol* 121:201–212, 1998
27. Foufelle F, Ferre P: New perspectives in the regulation of hepatic glycolytic and lipogenic genes by insulin and glucose: a role for the transcription factor sterol regulatory element binding protein-1c. *Biochem J* 366:377–391, 2002
28. Niswender KD, Shiota M, Postic C, Cherrington AD, Magnuson MA: Effects of increased glucokinase gene copy number on glucose homeostasis and hepatic glucose metabolism. *J Biol Chem* 272:22570–22575, 1997
29. Ferre T, Riu E, Franckhauser S, Agudo J, Bosch F: Long-term overexpression of glucokinase in the liver of transgenic mice leads to insulin resistance. *Diabetologia* 46:1662–1668, 2003
30. Mourrieras F, Foufelle F, Foretz M, Morin J, Bouche S, Ferre P: Induction of fatty acid synthase and S14 gene expression by glucose, xylitol and dihydroxyacetone in cultured rat hepatocytes is closely correlated with glucose 6-phosphate concentrations. *Biochem J* 326:345–349, 1997
31. Fajas L, Auboeuf D, Raspe E, Schoonjans K, Lefebvre AM, Saladin R, Najib J, Laville M, Fruchart JC, Deeb S, Vidal-Puig A, Flier J, Briggs MR, Staels B, Vidal H, Auwerx J: The organization, promoter analysis, and expression of the human PPARgamma gene. *J Biol Chem* 272:18779–18789, 1997
32. Boelsterli UA, Bedoucha M: Toxicological consequences of altered peroxisome proliferator-activated receptor gamma (PPARgamma) expression in the liver: insights from models of obesity and type 2 diabetes. *Biochem Pharmacol* 63:1–10, 2002
33. Gavrilova O, Haluzik M, Matsusue K, Cutson JJ, Johnson L, Dietz KR, Nicol CJ, Vinson C, Gonzalez FJ, Reitman ML: Liver peroxisome proliferator-activated receptor gamma contributes to hepatic steatosis, triglyceride clearance, and regulation of body fat mass. *J Biol Chem* 278:34268–34276, 2003
34. Matsusue K, Haluzik M, Lambert G, Yim SH, Gavrilova O, Ward JM, Brewer B Jr, Reitman ML, Gonzalez FJ: Liver-specific disruption of PPARgamma in leptin-deficient mice improves fatty liver but aggravates diabetic phenotypes. *J Clin Invest* 111:737–747, 2003
35. Norris AW, Chen L, Fisher SJ, Szanto I, Ristow M, Jozsi AC, Hirshman MF, Rosen ED, Goodyear LJ, Gonzalez FJ, Spiegelman BM, Kahn CR: Muscle-specific PPARgamma-deficient mice develop increased adiposity and insulin resistance but respond to thiazolidinediones. *J Clin Invest* 112:608–618, 2003

36. Bergman RN, Ader M: Free fatty acids and pathogenesis of type 2 diabetes mellitus. *Trends Endocrinol Metab* 11:351–356, 2000
37. Shimada M, Shimano H, Gotoda T, Yamamoto K, Kawamura M, Inaba T, Yazaki Y, Yamada N: Overexpression of human lipoprotein lipase in transgenic mice: resistance to diet-induced hypertriglyceridemia and hypercholesterolemia. *J Biol Chem* 268:17924–17929, 1993
38. Kim JK, Fillmore JJ, Chen Y, Yu C, Moore IK, Pypaert M, Lutz EP, Kako Y, Velez-Carrasco W, Goldberg IJ, Breslow JL, Shulman GI: Tissue-specific overexpression of lipoprotein lipase causes tissue-specific insulin resistance. *Proc Natl Acad Sci U S A* 98:7522–7527, 2001
39. Levak-Frank S, Radner H, Walsh A, Stollberger R, Knipping G, Hoefler G, Sattler W, Weinstock PH, Breslow JL, Zechner R: Muscle-specific overexpression of lipoprotein lipase causes a severe myopathy characterized by proliferation of mitochondria and peroxisomes in transgenic mice. *J Clin Invest* 96:976–986, 1995
40. Starnes JW: Introduction to respiratory control in skeletal muscle. *Med Sci Sports Exerc* 26:27–29, 1994
41. Van Hinsbergh VW, Veerkamp JH, Van Moerkerk HT: Cytochrome c oxidase activity and fatty acid oxidation in various types of human muscle. *J Neurol Sci* 47:79–91, 1980
42. Jacobs AE, Oosterhof A, Veerkamp JH: Palmitate oxidation and some enzymes of energy metabolism in human muscles and cultured muscle cells. *Int J Biochem* 19:1049–1054, 1987
43. Kramer R: Structural and functional aspects of the phosphate carrier from mitochondria. *Kidney Int* 49:947–952, 1996
44. Tsuboyama-Kasaoka N, Tsunoda N, Maruyama K, Takahashi M, Kim H, Cooke DW, Lane MD, Ezaki O: Overexpression of GLUT4 in mice causes up-regulation of UCP3 mRNA in skeletal muscle. *Biochem Biophys Res Commun* 258:187–193, 1999
45. Cline GW, Vidal-Puig AJ, Dufour S, Cadman KS, Lowell BB, Shulman GI: In vivo effects of uncoupling protein-3 gene disruption on mitochondrial energy metabolism. *J Biol Chem* 276:20240–20244, 2001
46. Holloszy JO, Coyle EF: Adaptations of skeletal muscle to endurance exercise and their metabolic consequences. *J Appl Physiol* 56:831–838, 1984
47. Nisoli E, Clementi E, Moncada S, Carruba MO: Mitochondrial biogenesis as a cellular signaling framework. *Biochem Pharmacol* 67:1–15, 2004
48. Lin J, Wu H, Tarr PT, Zhang CY, Wu Z, Boss O, Michael LF, Puigserver P, Isotani E, Olson EN, Lowell BB, Bassel-Duby R, Spiegelman BM: Transcriptional co-activator PGC-1 alpha drives the formation of slow-twitch muscle fibres. *Nature* 418:797–801, 2002
49. Kamei Y, Ohizumi H, Fujitani Y, Nemoto T, Tanaka T, Takahashi N, Kawada T, Miyoshi M, Ezaki O, Kakizuka A: PPARgamma coactivator 1beta/ERR ligand 1 is an ERR protein ligand, whose expression induces a high-energy expenditure and antagonizes obesity. *Proc Natl Acad Sci U S A* 100:12378–12383, 2003
50. Abu-Elheiga L, Oh W, Kordari P, Wakil SJ: Acetyl-CoA carboxylase 2 mutant mice are protected against obesity and diabetes induced by high-fat/high-carbohydrate diets. *Proc Natl Acad Sci U S A* 100:10207–10212, 2003